JOURNAL OF BACTERIOLOGY, Nov. 1987, p. 5231–5240
0021-9193/87/115231-10$02.00/0

Vol. 169, No. 11

Initiation of Chromosome Replication in Bacteria: Analysis of an Inhibitor Control Model

H. MARGALIT† AND N. B. GROVER*

The Hubert H. Humphrey Center for Experimental Medicine and Cancer Research, Hebrew University-Hadassah Medical School, Jerusalem 91010, Israel

Received 6 April 1987/Accepted 24 July 1987

This article contains an analysis of a version of the well-known inhibitor-dilution model for the control of initiation of chromosome replication in bacteria. According to this model, an unstable inhibitor interacts with an initiation primer in a hit-and-destroy fashion to prevent successful initiation; both constituents are presumed to be RNA species that are synthesized constitutively. The model further postulates that the inhibitor interacts cooperatively with the primer, that the inhibitor gene is removed some distance from the origin of replication, and that an eclipse period exists during which the chromosome origin is not able to reinitiate. This unstable-inhibitor version is characterized by four parameters: the inhibitor half-life, the cooperativity index, the location of the inhibitor gene, and the eclipse period; computer simulations are used to study the effect of each of these on the DNA and interdivision time distributions in exponentially growing steady-state cultures. In neither case was any combination of parameter values found that could provide even moderately satisfactory agreement between the simulation results and experimental data. From the examples furnished and the associated discussion, it appears that there are none—that no combination of parameter values exists that can reasonably be expected to produce a significantly better fit than those tested. We conclude that the model in its present form cannot be a valid description of chromosome replication control in bacteria. It is pointed out that this does not necessarily apply to negative initiation control models in general, or even to all inhibitor-dilution systems, merely to the particular ColE1-like mechanism considered here. Nevertheless, recent experimental results, which can only be understood in terms of a very high degree of initiation synchrony within individual cells, offer strong evidence against stochastic models of this kind for the control of chromosome replication.

At any fixed temperature, bacteria in steady-state exponential growth have different average generation times, depending on the composition of the culture medium. Since the duration of chromosome replication and the interval between its termination and the subsequent cell division are both essentially constant, the major contribution to this difference must come from the timing of the initiation event itself (18).

The initiation of chromosome replication is thus a critical stage in the cell cycle of bacteria, and despite the considerable experimental data available regarding replication at different growth rates, the precise factors responsible for its control remain largely unknown.

Originally it was thought that initiation occurs when a fixed ratio is attained between cell mass and the number of origins of replication, independent of the growth rate (5; R. H. Pritchard, Heredity **23**:472–473, 1968), and although more recent studies may have cast some doubt on the precise quantitative nature of this relationship (3), the concept of a property related to cell mass controlling initiation remains valid and continues to serve as the basis for models of the regulatory process. These fall into two main classes: those in which initiation is repressed by an inhibitor that is diluted owing to cell growth until its concentration per origin falls below a critical level, at which point initiation occurs (24), and those that require a fixed amount of initiator substance per origin, an initiation structure, in order for initiation to take place (5, 10).

In a previous article (16), we presented a detailed quantitative analysis of the initiation structure model originally put forward by Sompayrac and Maaløe (29) and were able to delineate the characteristics that such a control system would need to possess to be capable of regulating chromosome replication. We now turn our attention to the other type of mechanism, the so-called unstable-inhibitor or negative-control system. We shall confine ourselves to one particular form of the model only, that patterned after the regulation of copy number in the multicopy plasmid ColE1, since it is the most explicit ever published (23), but it should be borne in mind that the original version (24) is far more general in scope and hence less readily testable; our conclusions, therefore, will be limited accordingly.

The ColE1-like version of the model is probabilistic in nature and so we have chosen a simulation approach: computer representations of individual cells grow and divide according to the specifications of the model; testing is carried out by comparing predicted and observed distributions, rather than average values. We conclude that the unstable-inhibitor model in the form considered here is unable to explain the regulation of chromosome replication in bacteria.

MATERIALS AND METHODS

Symbols. The following symbols are used in this paper: a, cell age (minutes); a_d, age at which inhibitor genes replicated (minutes); a_j, age at which jth copy of gene replicated (minutes); C, time required for replication fork to traverse genome (minutes); D, time between end of a round of replication and subsequent cell division (minutes); g, inhibitor genes (number per cell); k, constant of proportionality; k_1, rate of primer transcription (molecules per gene per min);

* Corresponding author.
† Present address: Laboratory of Mathematical Biology, National Cancer Institute, Bethesda, MD 20892.

k_2, rate of inhibitor synthesis (molecules per gene per min); k_3, rate of inhibitor degradation (per minute); k', kk_1; P, probability of initiation of chromosome replication (number/Δt); r, inhibitor molecules (number per cell); t, time (minutes); V, cell volume (cubic micrometers); Δt, step size (minutes); ε, duration of eclipse period (minutes); λ, inhibitor half-life (minutes); ν, cooperativity index (number); ξ, locus of inhibitor gene (fraction of C); τ, interdivision time (minutes); and $\bar{\tau}$, doubling time of culture (minutes).

The model. A variant of the inhibitor-dilution model also proposed by Pritchard et al. in their 1969 article, that of the unstable inhibitor, has undergone considerable revision and development since then, in effect superceding the original version and becoming the negative-control model of choice (22, 23).

The main component of the unstable-inhibitor model as it now stands (23) is an inhibitor of initiation that is synthesized constitutively and is unstable. To sharpen the dependence of the probability of initiation on the inhibitor concentration, the inhibitor is considered to interact cooperatively with its target. It then becomes necessary to impose a delay between an initiation event and the subsequent rise in inhibitor concentration resulting from the replication of the inhibitor gene, so as to maintain an acceptable level of initiation synchrony within individual cells containing more than one chromosome origin. The inhibitor gene is therefore placed some distance from the origin of replication. Finally, to decrease the probability of one origin replicating twice before another in the same cell has replicated once, the existence of an eclipse period after initiation is postulated during which an origin is not capable of reinitiation; to be effective, this eclipse period needs to be longer than the time interval between initiation and replication of the control gene.

In at least one group of plasmids, represented by ColE1, initiation of replication is under the control of a constitutively synthesized unstable inhibitor. This is a small untranslated RNA, and its target is the RNA primer of initiation; inactivation is effected by binding to a region of the primer having a common base sequence (26). There is no evidence that this inhibitor-primer interaction is cooperative, but of course such a property is not expected in plasmids in which replication occurs randomly throughout the cell cycle (19).

For the sake of concreteness, we will assume in the present analysis that both the inhibitor and its target are RNA molecules and that the latter is synthesized constitutively as well.

Basic equations. The unstable-inhibitor model states that the probability P of chromosome initiation at an origin of replication is directly proportional to the rate of primer transcription k_1 and inversely proportional to some power ν of the inhibitor concentration $[r]$: $P = kk_1/[r]^\nu$, where k is the constant of proportionality and ν is the cooperativity index. Since the primer is considered to be synthesized constitutively, k_1 is independent of cell age at any given growth rate and temperature, and the product kk_1 can be replaced by a single constant k':

$$P = k'/[r]^\nu. \tag{1}$$

The inhibitor r is also produced constitutively and is unstable so that its net rate of synthesis is given by (16, 29)

$$dr\,(a)/d(a) = k_2 g(a) - k_3 r(a) \tag{2}$$

where a denotes cell age, $g(a)$ is the number of inhibitor genes, and k_2 and k_3 are constants representing the rates of transcription and degradation of the inhibitor, respectively. In synchronously replicating sister chromosomes, the cell cycle can be divided into two intervals, before and after gene doubling, and equation 2 can be integrated separately over each to yield

$$\begin{aligned} r(a) &= r(0)e^{-k_3 a} + g(0)(1 - e^{-k_3 a})k_2/k_3 && \text{for } 0 \le a \le a_d \\ &= r(a_d)e^{-k_3(a - a_d)} + 2g(0)(1 - e^{-k_3(a - a_d)})k_2/k_3 && \text{for } a_d \le a \le \bar{\tau} \end{aligned} \tag{3}$$

Here a_d is the age at which the inhibitor genes are replicated, and $\bar{\tau}$ is the doubling time of the culture.

A basic feature of the present model, however, is its stochastic nature: replications within a cell are not synchronous, and different copies of a gene are duplicated at different times during the cell cycle. This necessitates modifying equation 3:

$$r(a) = r(a_j)e^{-k_3(a - a_j)} + g(a)(1 - e^{-k_3(a - a_j)})k_2/k_3 \quad \text{for } a_j \le a \le a_{j+1} \tag{4}$$

where $a_0 \equiv 0$ and $a_j (j \ge 1)$ is the age of the cell at which the jth copy of the gene duplicates.

Equations 1 and 4 form the basis for our simulations.

Computer simulation. The unstable-inhibitor model contains several independent parameters: the cooperativity index ν, the locus of the inhibitor gene ξ, the duration of the eclipse period ε, and the inhibitor half-life λ; a different simulation run is required for every unique combination. (Details concerning the actual values used for each of the parameters appear below.) In addition, there are two adjustable constants, k' and k_2.

We begin the simulation with a homogeneous population of cells and arbitrary starting values for the constants. At each time step, a proportion P of the cells undergo initiation, as specified by equation 1 with r taken from equation 4; when there is more than one origin of replication in a cell, each available origin (one in which the time since the previous initiation exceeds the eclipse period) is assigned equal probability. In principle, all available origins can initiate replication during any given time interval Δt. In practice, the chances of more than one actually doing so are exceedingly small, too small to justify the additional programming effort required to deal with it; initiations within a single cell were therefore arbitrarily limited to one per interval. In successive intervals, however, additional origins can, and do, initiate, subject to their availability and to the same probabilities mentioned above. Thus, after a while, a rather diverse assortment of chromosome configurations arises in the different cells (Fig. 1). Division into daughter cells of nearly equal size (see below) occurs when the age of the oldest replication fork reaches $C+D$ min, where C is the time required for a replication fork (pair of forks, really, since replication is bidirectional) to traverse the genome and D is the time between the end of a round of replication and the subsequent cell division.

The constants k' and k_2 are adjusted until the total number of origins in the culture and the total number of inhibitor

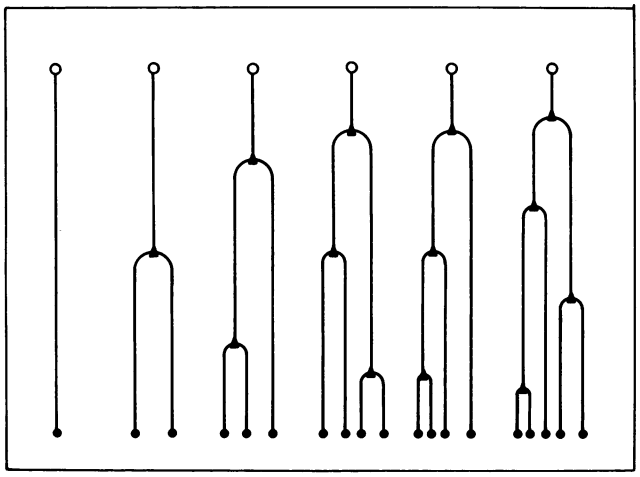

FIG. 1. Schematic representation of more common chromosome configurations within bacterial culture in steady-state exponential growth when initiation of chromosome replication is regulated according to unstable-inhibitor control model. Chromosomes are represented as linear, rather than circular, structures and replication as a unidirectional, rather than bidirectional, process for reasons of clarity. Symbols: ●, origin of replication; ▲, replicating fork; ○, terminus.

RNA molecules exactly double every τ min; as expected, the final values of k' and k_2 are independent of their starting values for any given set of model parameters. Having established exponential growth, we now proceed with the simulation until steady-state balanced growth is reached, as indicated by the distributions of various extensive quantities, such as cell volume, DNA content, and number of inhibitor RNA molecules per cell, becoming time invariant. The calculations are executed in an iterative fashion so that when balanced growth is achieved, it is also exponential. A flow chart illustrating the major steps in the simulation process is presented in Fig. 2.

Five quantities are used to classify the cells during the simulation. Three of these, time at last division, cell volume, and number of inhibitor molecules, refer to the state of the cell at birth; the other two, chromosome configuration and age of each replication fork, change with cell age. Ideally, cells should be looked upon as identical only when all five quantities are precisely the same. To keep the problem tractable, however, a small compromise had to be made: cells whose volumes and inhibitor content at birth did not differ by more than 3% were considered indistinguishable, provided the other three quantities were indeed identical.

We return now to the question of cell division. Chromosome segregation is taken to be random, except that no DNA-less daughter cells are permitted. The volume of newborn cells is treated as a normally distributed random variable with a coefficient of variation of 8.1% (34); the inhibitor concentration is assumed not to change during cell division.

Parameter values. All simulations were carried out for a doubling time $\bar{\tau}$ of 60 min in steps Δt of 4 or 6 min, except when technical restrictions necessitated using 8-min increments (see below).

The adjustable constants k' and k_2 were set in accordance with the requirements of exponential growth, as described above. The rate of inhibitor RNA degradation k_3 is more conveniently discussed in terms of the inhibitor half-life λ, where $\lambda = \ln 2/k_3$. The model specifies that the inhibitor molecules be unstable but of course does not state to what extent. The average mRNA half-life in a cell is 1.3 min (20), and so we chose λ values of 0.2, 1.3, and 7.5 min, corresponding to a highly labile, an average, and a relatively stable species.

To sharpen the dependence of the probability of initiation on the inhibitor concentration, the inhibitor is considered to interact cooperatively with the primer. The number of inhibitor molecules that participate jointly in the inhibitor-primer interaction is termed the cooperativity index ν. We used a lower limit of 1, which is equivalent to no cooperativity at all, and an upper limit of 20.

The model places the inhibitor gene some distance from the chromosome origin to maintain an acceptable level of initiation synchrony within individual cells. Three different values for this delay time ξ were used: 0.10, 0.25, and 0.50, corresponding to 1/10 the time it takes to replicate a chromosome, 1/4, and 1/2.

Finally, to decrease the probability of an origin replicating a second time before its sister origin replicates once, the existence of an eclipse period after initiation was postulated during which an origin is not capable of reinitiation. To be effective, this eclipse period ε needs to be longer than the time interval between initiation and replication of the inhibitor gene, ξC. The literature does not contain much quantitative data on ε. An early estimate in a *thy* mutant strain after prolonged thymine starvation (36) gave a lower limit of 12 min, but the irreversible effects of thymine starvation on the rate of DNA synthesis make any measurement based on such a system suspect. More recent data using temperature-sensitive initiation-defective replication mutants (17) suggest an eclipse period of about 20 min at 30°C. Density shift experiments with a doubling time $\bar{\tau}$ of 78 min produce a much higher value, 54 min at 30°C (13). Since ε cannot, of course, ever be greater than τ, such a large value suggests that ε is not constant but rather decreases with increasing growth rate (or temperature). If one assumes $\varepsilon \propto \bar{\tau}$, this implies a value of 40 to 45 min at $\bar{\tau} = 60$ min. In the end, we decided on 20, 30, and 40 min.

These values for ε and the other independent parameters of the model are shown in Table 1, for ease of reference. In addition, several simulation runs were carried out at $\varepsilon = 8$ min but with reduced sensitivity (increased step size), because of technical limitations.

The time required for a replication fork to traverse the genome, C, and the time between the end of a round of replication and the subsequent cell division, D, were assigned their usual values of 40 and 20 min, respectively (11); the average volume of newborn cells was taken to be 0.3 μm^3 (25).

RESULTS

The unstable-inhibitor model was simulated for every combination of parameter values shown in Table 1 and for several others to be discussed below, as described in the preceding section and illustrated schematically in Fig. 2.

Once exponential growth had been attained, the distributions of cell volume, DNA content, and number of inhibitor molecules per cell at a particular time t were compared with those at a slightly later time, typically $t+4\Delta t$, where Δt is the simulation step size. Only when the residuals for each of these three variables were found to be randomly distributed ($P > 0.20$) by all the statistical tests used (runs test, sign test, and serial correlation test), did we consider steady-state balanced growth to have been attained; the iterations were

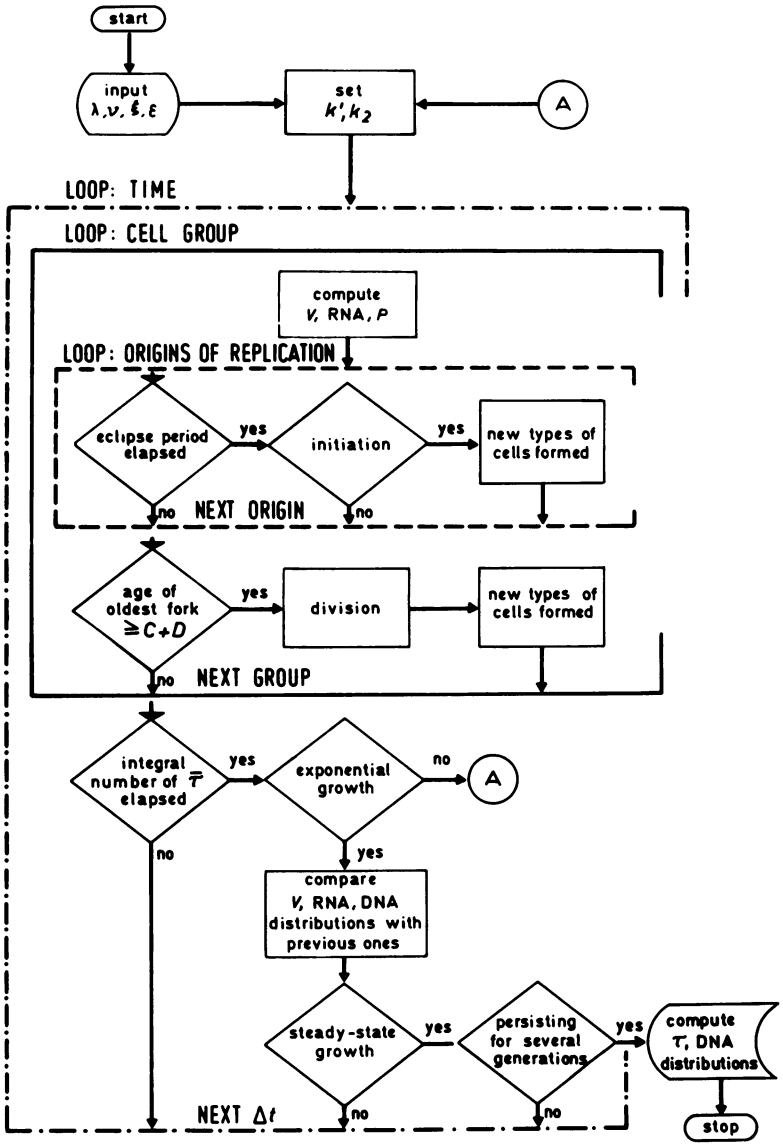

FIG. 2. Major steps in simulation of unstable-inhibitor control model.

allowed to proceed beyond this point for several additional time periods, during which the statistical testing was repeated, just to make sure that convergence had indeed been achieved. All simulations attempted ran to completion, as judged by these criteria, but took different amounts of simulated biological time to do so. Figure 3 shows an example of the quality of convergence obtained. In this case, steady-state balanced growth was reached during generation 16 after the onset of exponential growth and the data are from generation 17. The statistical analysis appears in the caption.

All the usual validation procedures were carried out, including checking the mean DNA content per cell and the mean number of origins against expected values (2, 11) and making sure that the total number of cells and the total cell volume double every $\bar{\tau}$ minutes.

The probabilistic nature of the proposed control mechanism gives rise to a large variety of chromosome replication patterns (Fig. 4). Note the considerable spread in frequencies among the various configurations, the most common by far being the ones bearing closest resemblance to those predicted by the idealized cell cycle model of Cooper and Helmstetter (4).

Models are normally tested by comparing their predictions with the corresponding empirical entity. Here we have chosen (steady-state exponential growth) distributions rather than average values (16), as befits the stochastic nature of the model under study, testing both the interdivision time τ and the DNA content per cell. These two variables were selected because they can be expected to be sensitive to the particular properties of the model and

TABLE 1. Parameter values

Parameter	Values used
Inhibitor half-life (λ)	0.2, 1.3, 7.5 min
Cooperativity index (ν)	1, 5, 20
Gene locus (ξ)	1/10, 1/4, 1/2 *C*
Eclipse period (ϵ)	20, 30, 40 min

because in each case reliable experimental distributions, based on large numbers of cells, are available. The DNA data were obtained by flow cytometry (1, 15, 30–32) and consisted of measurements on over 250,000 cells of *Escherichia coli* B/r from a culture with a doubling time of 60 min; the raw data were kindly provided by K. Skarstad. The τ distributions were constructed from the observations of Harvey and Plank (7, 21), who used a method of analysis developed by Harvey (6, 8) to show that the interdivision time of *E. coli* B/r cells is normally distributed over a large range of growth rates with a coefficient of variation near 22%.

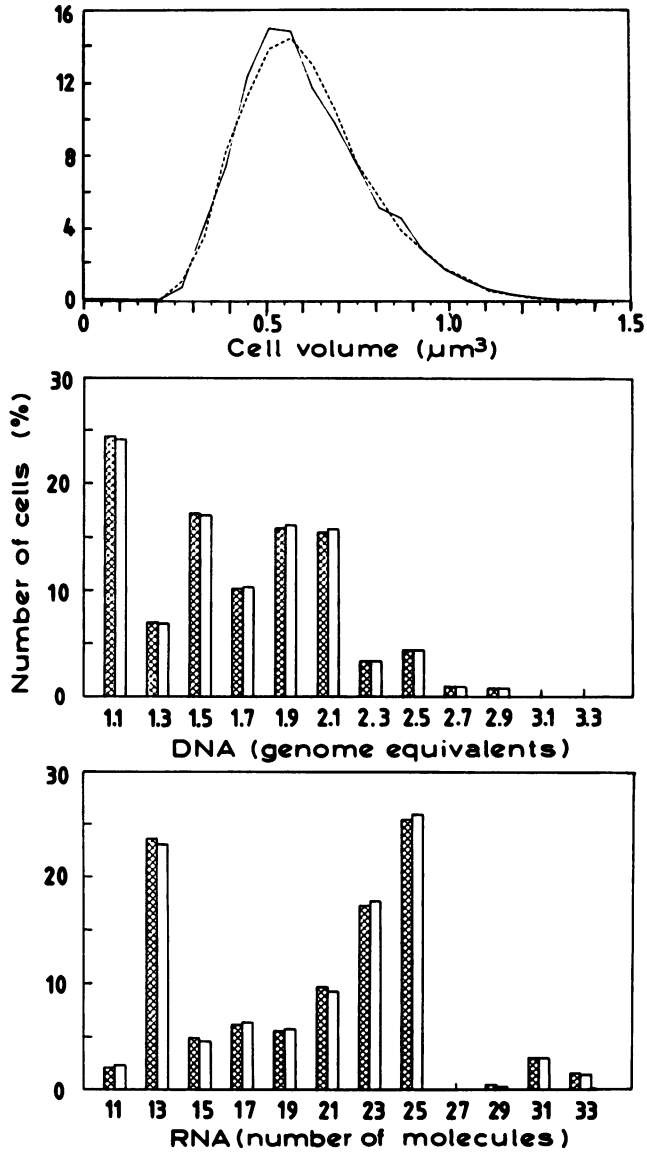

FIG. 3. Convergence to steady-state exponential growth. DNA and RNA distributions are presented as histograms because they are visually indistinguishable when plotted as continuous curves. Abscissae of histograms represent median values. Plots show distributions 17 generations after exponential growth was attained (—— and ▩) and 24 min later (– – – and □). Parameter values: λ = 7.5 min, ν = 5, ξ = 1/4, ε = 30 min. By the runs test, sign test, and serial correlation test, the probability that the differences are due to chance were, respectively, 0.851, 0.937, and 0.999 for cell volume, 0.588, 0.943, and 0.504 for DNA, and 0.400, 0.788, and 0.702 for RNA.

The enormous numbers of individual cells measured requires us to consider the experimental results as more properly describing a population, rather than a random sample. That being the case, hypothesis testing is not appropriate, and we have to resort to visual comparisons between the predicted and observed distributions: the model is (tentatively) accepted if there exists at least one combination of parameter values that looks able to provide a satisfactory fit to both the DNA and τ data; otherwise, it is rejected.

First we examine the τ distributions, an example of which is shown in Fig. 5. The convention adopted here and throughout the remainder of this article is that the experimental distributions (normal for τ, with a standard deviation of 13.2 min; empirical for DNA, with a sample size of about 260,000) are drawn as continuous curves, whereas the simulation results are presented in the form of histograms. The agreement can be seen to be quite poor, considering that we are comparing populations with the same mean.

The influence of the various parameters on the simulation results is displayed in Fig. 6. The values and layout were chosen to facilitate examination of the effect of each parameter separately, the experimental distribution being the same in all panels. (The center panel is a reproduction of Fig. 5 on a reduced scale.) Thus, the three middle panels (d, e, and f) illustrate the effect of increasing ν, since all the other parameters are held constant, while the center panels (b, e, and h) show what happens when we change ε; similarly, the positive diagonal (g, e, and c) is an example of the effect of λ and the negative diagonal (a, e, and i) shows the effect of ξ.

Consider first the cooperativity index ν, introduced to sharpen the dependence of the probability of initiation on the inhibitor concentration r/V, where V is the cell volume. That ν does indeed have the desired effect is clear, the coefficient of variation decreasing from 37.8% at ν = 1 to 29.8% at ν = 5 to 21.9% at ν = 20, this last being just below the experimental value of 22%. But even moderate levels of cooperativity have another, less obvious effect. Initiation will not occur until V is numerically very near r. (The latter is known only up to a constant of proportionality, its rate of synthesis k_2, and so one must compare apparent numerical values of V and r.) Since the inhibitor is unstable, its level in the cell will follow its gene dose rather closely. Thus, a cell with a chromosome configuration like the one pictured beneath the central bar of the first panel in Fig. 4 will have initiated replication at a volume corresponding to the amount of inhibitor produced by two genes. At division, the daughter cells will be of equal volume (more or less) and receive the same concentration of inhibitor but not the same number of genes. In the daughter cell with two gene copies, the rate of synthesis of the inhibitor will exceed the rate of degradation and its concentration will rise rapidly until it corresponds to the level produced by two genes; conversely, in the other daughter cell, the amount of inhibitor will fall until it reaches the level produced by a single gene copy. Thus, in the former, the next initiation can be expected to occur at about the same volume as in the preceding generation, so that the interdivision time will be close to average, whereas in the latter, initiation will occur much earlier, resulting in a τ that is well below $\bar{\tau}$. Since the configuration we are considering makes up about 10% of the entire population (Fig. 4), the model gives rise to a disproportionately large number of cells with short interdivision times.

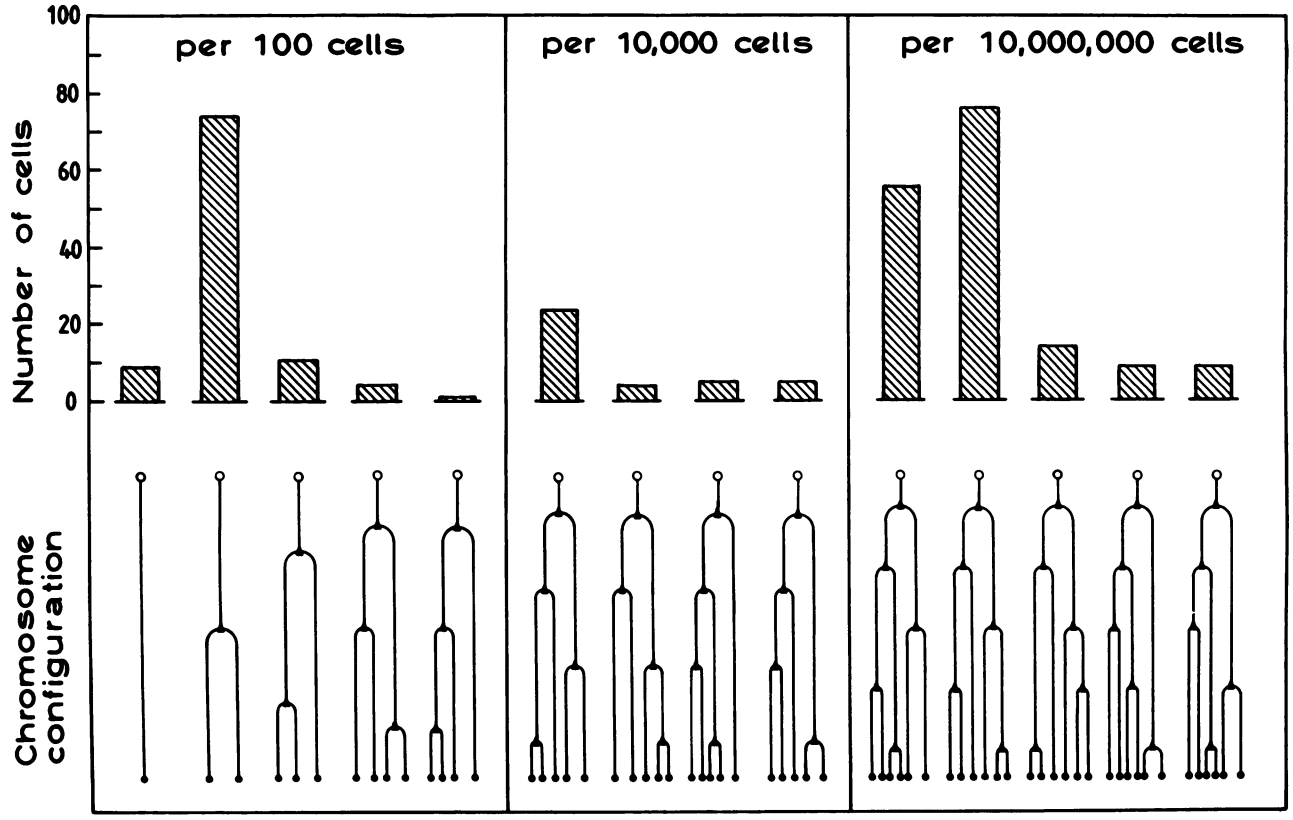

FIG. 4. Distribution of chromosome configurations in culture during steady-state exponential growth. Chromosomes are represented as linear, rather than circular, structures, and replication is shown as a unidirectional, rather than bidirectional, process for reasons of clarity. Note use of three different scale factors. Symbols: ●, origin of replication; ▲, replicating fork; ○, terminus. Parameters: $\lambda = 1.3$ min, $\nu = 5$, $\xi = 1/10$, $\varepsilon = 20$ min.

Thus, when there is no cooperativity (Fig. 6d), interdivision times are too disperse, but as ν is increased, not only does the τ distribution become narrower, as expected, its tails also contract, the upper one more than the lower (Fig. 6e), so that by the time the coefficient of variation is about right (Fig. 6f), the distribution itself is strongly platykurtic and has a considerable negative skew. In all cases, however, the actual shape of the lower tail is determined by ε. The eclipse period does not directly affect inhibitor synthesis and degradation (as do ξ and λ, respectively) or the sensitivity of initiation to inhibitor concentration (as does ν). What it does do, primarily, is to prevent successive initiations from occurring too close to one another at the same origin. This is perhaps the most striking feature of Fig. 6 (other than the obvious uniform lack of fit, of course): since the interdivision time of a cell cannot be less than ε, the lower tail of the distribution shifts to the right as ε is raised, its height increasing in the process to accommodate those cells that would otherwise have had $\tau < \varepsilon$.

As the stability of the inhibitor is raised, the number of inhibitor molecules per cell will no longer be proportional to gene dose but will increase slowly with cell age. Inhibitor concentration, therefore, will change less rapidly with cell age and so will the probability of initiation. The result is an increase in the coefficient of variation of the τ distribution with increasing λ. The further the inhibitor gene is from the origin of replication (the larger the value of ξ), the more time there is available for the second sister origin in a pair to undergo initiation before the fork from the first replicates the

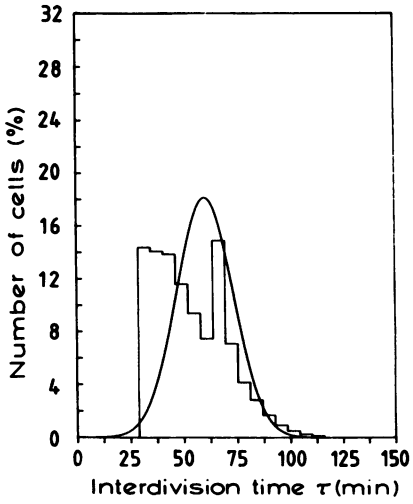

FIG. 5. Comparison between experimental and predicted interdivision time distributions. The curve shows experimental data, constructed from observations of Harvey and Plank (7, 21), and the histogram shows predictions of the model. Parameters: $\lambda = 1.3$ min, $\nu = 5$, $\xi = 1/4$, $\varepsilon = 30$ min.

gene and so raises the inhibitor concentration; this will cause an increase in the skew of the distribution. Usually, both these effects are minor (Fig. 6). But when gene duplication occurs near the end of the eclipse period, this is no longer the case; rather, the simulation results become very sensitive to the particular values chosen for λ and ξ. For small values of the ratio $(\varepsilon - \xi C)/\lambda$, the inhibitor level at the end of the eclipse period, when all origins are again available for initiation, will not be sufficient to inhibit further initiation. The result will be a burst of initiation after the sudden increase in the number of accessible origins, giving rise to large numbers of cells with very short interdivision times (Fig. 7) and complex chromosome configurations of the type illustrated by the last panel in Fig. 4.

It is clear from Fig. 6 and 7 and the above discussion that other combinations of parameter values, either within the range covered by Fig. 6 or beyond, would not materially improve the fit between the simulation results and the experimentally derived distribution.

We now turn to the DNA data. Figure 8 compares the experimental results with those produced by computer simulation with the same combination of parameter values as in Fig. 5, and Fig. 9 (like Fig. 6) shows the effects of changing the various parameters one at a time. Other than a decrease in the width and asymmetry of the distribution caused by an increase in ν or ε, especially the latter, the precise values of the parameters do not appear to influence the DNA distribution very much, far less than for the corresponding τ distribution. Such insensitivity implies that the poor quality of the fit seen in Fig. 9 will persist whatever the parameter values.

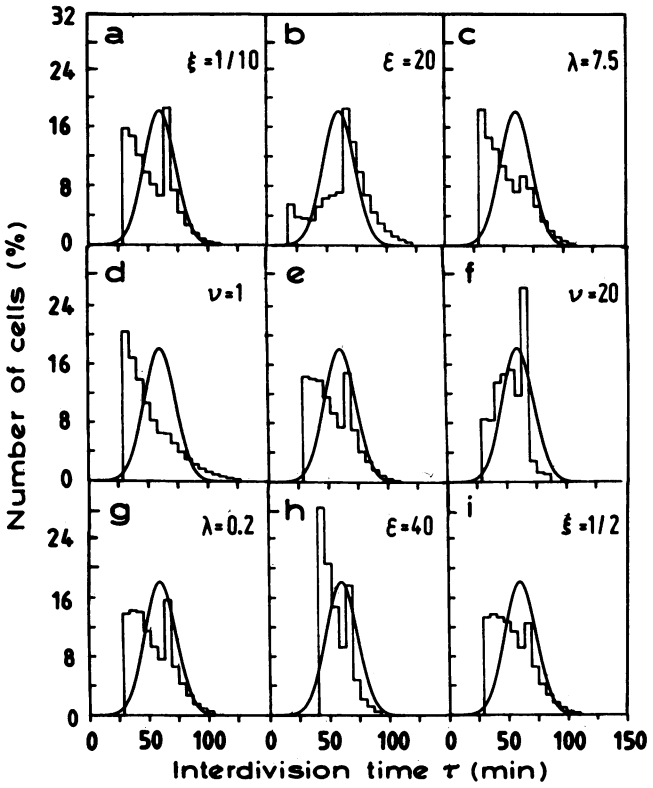

FIG. 6. Effect of parameters on interdivision time distribution. The curves (same one in each panel) show experimental data, constructed from observations of Harvey and Plank (7, 21), and the histograms (different in the different panels, depending on parameter values) show predictions of the model. Parameters (except where indicated otherwise in figure): λ = 1.3 min, ν = 5, ξ = 1/4, ε = 30 min.

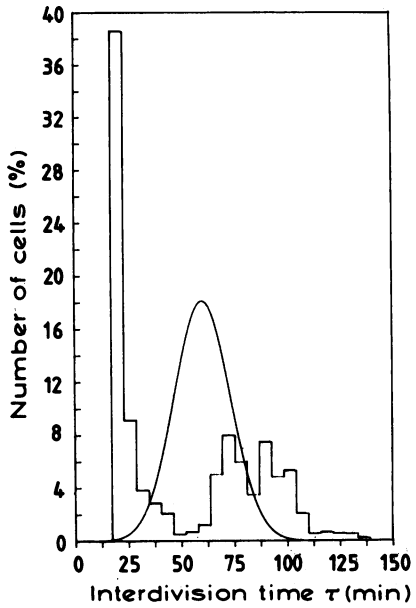

FIG. 7. Comparison between experimental and predicted interdivision time distributions with duplication of inhibitor gene at end of eclipse period. The curve shows experimental data, constructed from observations of Harvey and Plank (7, 21), and the histogram shows predictions of the model. Parameters: λ = 7.5 min, ν = 20, ξ = 1/2, ε = 20 min.

Both the DNA and the τ distributions were tested for all combinations of parameter values shown in Table 1, and in every case, there were large and obvious discrepancies between the simulation results and the experimental data for at least one of the variables. In addition, as mentioned before, several simulations were carried out with a short eclipse period, 8 min. Because of technical difficulties, these

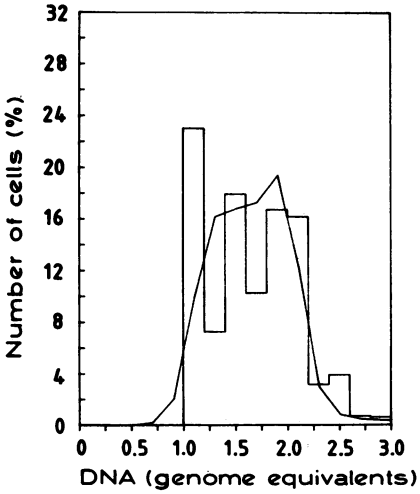

FIG. 8. Comparison between experimental and predicted DNA distributions. The curve shows experimental data, obtained by flow cytometry techniques (raw data kindly provided by K. Skarstad), and the histogram shows predictions of the model. Parameters: λ = 1.3 min, ν = 5, ξ = 1/4, ε = 30 min.

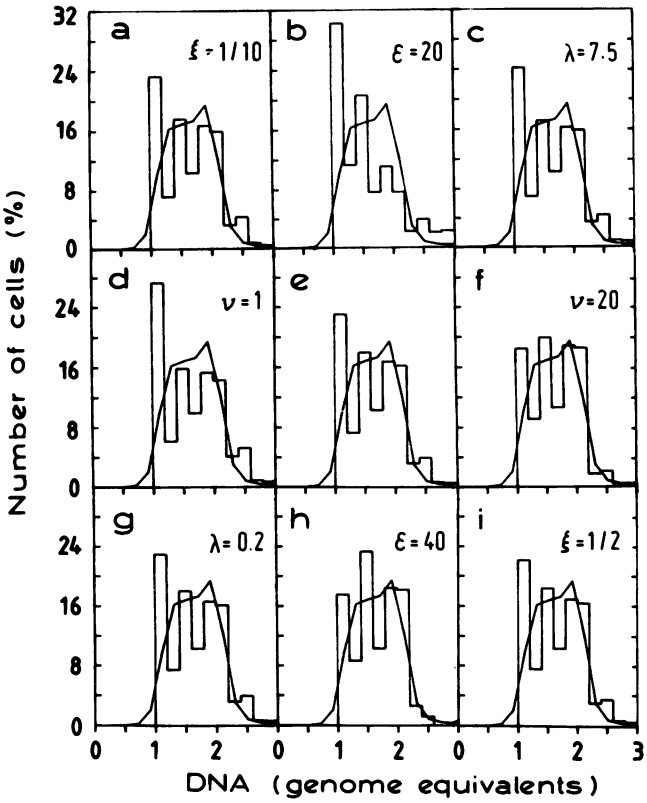

FIG. 9. Effect of parameters on DNA distribution. The curves (same one in each panel) show experimental data, obtained by flow cytometry techniques (raw data kindly provided by K. Skarstad), and the histograms (different in the different panels, depending on parameter values) show predictions of the model. Parameters (except where indicated otherwise in figure): $\lambda = 1.3$ min, $\nu = 5$, $\xi = 1/4$, $\varepsilon = 30$ min.

runs could only be executed with larger step sizes, 8 min instead of the usual 4 or 6. An example of such a simulation for $\varepsilon = 8$ min is shown in Fig. 10, with the other parameters as in Fig. 6a and 9a. The results are in accordance with the expected effect of ε on the distributions, as discussed in conjunction with Fig. 6 and 9, and are clearly highly unsatisfactory. (To make sure that increasing the step size does not introduce distortion, all simulations with $\varepsilon = 20$ were rerun with the larger step size. No discernible differences were detected, apart from the expected decrease in resolution.)

DISCUSSION

The earlier versions of the negative-control model proposed by Pritchard and colleagues (22, 24) anticipated conceptually many of the specific elements later found to make up actual regulatory systems in plasmids (26), and the model was subsequently reformulated in the light of these findings (23); additional properties were introduced to account for the differences between plasmid and chromosome replication (22, 23).

As it now stands, the unstable-inhibitor model is characterized by four parameters: the inhibitor half-life λ, the cooperativity index ν, the location of the inhibitor gene ξ, and the eclipse period ε. The effect of each one of these was investigated for every combination of the other three (Table 1), covering and exceeding the entire range implied by the model. Thus, inhibitor stability was varied from highly unstable ($\lambda = 0.2$ min) to relatively stable ($\lambda = 7.5$ min), cooperativity was varied from none at all ($\nu = 1$) to an unrealistically high level (20 inhibitor molecules per primer), the location of the inhibitor gene was varied from quite near the origin ($\xi = 1/10$) to halfway towards the terminus, and the eclipse period was varied from a value of 8 min, which is rather short, up to 40 min. (The latter is possible only if ε is an increasing function of τ since ε can never exceed the doubling time, and values of $\bar{\tau}$ down to 22 min or so are well established for *E. coli* B/r in steady-state exponential growth at 37°C.)

Each simulation was continued until steady-state exponential growth had been attained, as indicated by the distributions of cell volume, DNA content, and number of inhibitor molecules per cell all becoming time invariant; only then were comparisons made with the experimental data. These were of two kinds. The first, the interdivision time distribution, τ, was constructed from the observations of Harvey and Plank (7, 21), who showed that the τ of *E. coli* B/r is normal; the second, the empirical DNA distribution kindly provided by K. Skarstad, was obtained by flow cytometry techniques (1) and consisted of measurements on over 250,000 cells.

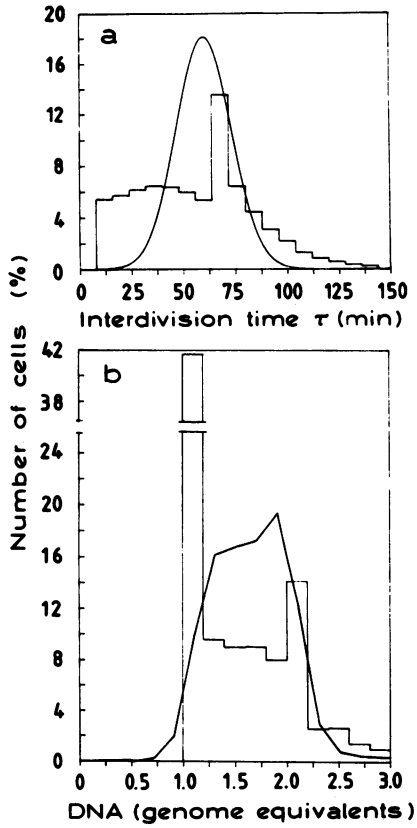

FIG. 10. Comparison between experimental and predicted distributions with a short eclipse period. Parameters: $\lambda = 1.3$ min, $\nu = 5$, $\xi = 1/10$, $\varepsilon = 8$ min. (a) Interdivision time distribution. The curve shows experimental data, constructed from observations of Harvey and Plank (7, 21), and the histogram shows predictions of the model. (b) DNA distribution. The curve shows experimental data, obtained by flow cytometry techniques (raw data kindly provided by K. Skarstad), and the histogram shows predictions of the model.

In neither case was any combination of parameter values found that could provide even moderately satisfactory agreement between the simulation results and the experimental data. From the examples furnished, and the associated discussion, it would appear that there are none, that no combination of parameter values exists that can reasonably be expected to produce a significantly better fit than those tested. We conclude that the model in its present form cannot be a valid description of chromosome replication control in bacteria.

A general problem with stochastic (as opposed to deterministic) models concerns their demands on computer resources. These tend to be quite substantial, even for modest simulations, and they increase very rapidly with decreasing step size. In the present context, making the step size smaller causes the number of different cell classes to rise sharply and considerably more computer memory (and processing time) is then required. Despite recourse to highly efficient packing and storing algorithms, we soon exceeded the ultimate capacity of our computer; the step size used here is the smallest one possible for this kind of study on the VAX-11/780. Nonetheless, it remains relatively large, and one cannot rule out the possibility that reducing it further would have improved the fit.

The interdivision time distributions predicted by the model are a direct reflection of the distributions of cell ages at initiation of chromosome replication, since the time interval between the latter event and cell division, $C+D$, was assumed to be the same for all cells regardless of their age and size at initiation. This may be an oversimplification. The reported correlation between length at cell constriction and length at initiation of replication is very high but not perfect (12), and whereas the observed decrease in cell radius during that period (35), coupled with the likelihood that cells control their surface area rather than their length (37), would imply an even stronger correlation as regards cell age, some influence of cell size at initiation on the length of the $C+D$ period cannot be ruled out completely. If any such effect does exist, however, it must be a very weak one and is not likely to affect the validity of our conclusions in any substantial way.

It should be pointed out that these conclusions do not necessarily apply to negative initiation control models in general, or even to all inhibitor-dilution systems, merely to the particular, ColE1-like mechanism (9, 14, 27, 33) considered here. Nevertheless, the recent experimental results of Skarstad et al. (28), which can only be understood in terms of a very high degree of initiation synchrony within individual cells, greater than 97% for *E. coli* B/r growing at $\bar{\tau} = 27$ min, argue strongly against stochastic models of this kind for the control of chromosome replication.

A few years ago (16), we carried out an analysis of the initiation structure model first put forward by Sompayrac and Maaløe (29) in which a protein whose concentration does not change much during the cell cycle serves as an initiator of chromosome replication in a control system consisting of a single operon coding for both the initiator and an autorepressor; the two species are synthesized in a fixed polarity, the transcription of the entire operon being controlled by the autorepressor itself. This is a deterministic, rather than stochastic, model and so, instead of simulating an entire population, it is sufficient to follow the behavior of a single representative cell. Unlike the present model, which we were forced to reject when no combination of parameter values could be found that produced acceptable agreement with the experimental data, it would appear that the autorepressor control model is capable of regulating chromosome replication, provided certain rather stringent requirements are met as regards the location of the operon (fairly near the origin of replication), the strength of its promoter (moderate to strong), the nature of the interaction between its operator and repressor (rather weak specific competitive binding), the effectiveness of the ribosome binding site on its mRNA transcript (below average), and the messenger half-life (not too long). We have now begun a study to determine whether the *dnaA* gene product possesses the requisite properties and is able to fulfill the roles of both initiator and autorepressor in such a system.

ACKNOWLEDGMENTS

We wish to thank Celia Eaglstein for her help in plotting the graphs.

This work was supported in part by the Harry and Abe Sherman Foundation and by a European Molecular Biology Organization long-term fellowship (to N.B.G.).

LITERATURE CITED

1. **Boye, E., H. B. Steen, and K. Skarstad.** 1983. Flow cytometry of bacteria: a promising tool in experimental and clinical microbiology. J. Gen. Microbiol. **129**:973–980.
2. **Churchward, G., H. Bremer, and R. Young.** 1982. Macromolecular composition of bacteria. J. Theor. Biol. **94**:651–670.
3. **Churchward, G., E. Estiva, and H. Bremer.** 1981. Growth rate-dependent control of chromosome replication initiation in *Escherichia coli*. J. Bacteriol. **145**:1232–1238.
4. **Cooper, S., and C. E. Helmstetter.** 1968. Chromosome replication and the division cycle of *Escherichia coli* B/r. J. Mol. Biol. **31**:519–540.
5. **Donachie, W. D.** 1968. Relationship between cell size and time of initiation of DNA replication. Nature (London) **219**:1077–1079.
6. **Harvey, J. D.** 1972. Synchronous growth of cells and the generation time distribution. J. Gen. Microbiol. **70**:99–107.
7. **Harvey, J. D.** 1972. Parameters of the generation time distribution of *Escherichia coli* B/r. J. Gen. Microbiol. **70**:109–114.
8. **Harvey, J. D.** 1983. Mathematics of microbial age and size distributions, p. 1–35. *In* M. Bazin (ed.), Mathematics in microbiology. Academic Press, Inc., New York.
9. **Hashimoto-Gotoh, T., and J. Inselburg.** 1979. ColE1 plasmid incompatibility: localization and analysis of mutations affecting incompatibility. J. Bacteriol. **139**:608–619.
10. **Helmstetter, C. E., S. Cooper, O. Pierucci, and E. Revelas.** 1968. On the bacterial life sequence. Cold Spring Harbor Symp. Quant. Biol. **33**:809–822.
11. **Helmstetter, C. E., O. Pierucci, M. Weinberger, M. Holmes, and M.-S. Tang.** 1979. Control of cell division in *Escherichia coli*, p. 517–546. *In* J. R. Sokatch and L. N. Ornston (ed.), The bacteria, vol. VII. Academic Press, Inc., New York.
12. **Koppes, L. J. H., and N. Nanninga.** 1980. Positive correlation between size at initiation of chromosome replication in *Escherichia coli* and size at initiation of cell constriction. J. Bacteriol. **143**:89–99.
13. **Koppes, L. J., and K. Nordström.** 1986. Insertion of an R1 plasmid into the origin of replication of the *E. coli* chromosome: random timing of replication of the hybrid chromosome. Cell **44**:117–124.
14. **Lacatena, R. M., and G. Cesareni.** 1983. Interaction between RNA1 and the primer precursor in the regulation of ColE1 replication. J. Mol. Biol. **170**:635–650.
15. **Lindmo, T., and H. B. Steen.** 1979. Characteristics of a simple, high-resolution flow cytometer based on a new flow configuration. Biophys. J. **28**:33–44.
16. **Margalit, H., R. F. Rosenberger, and N. B. Grover.** 1984. Initiation of DNA replication in bacteria: analysis of an autorepressor control model. J. Theor. Biol. **111**:183–199.
17. **Messer, W., U. Bellekes, and H. Lother.** 1985. Effect of *dam* methylation on the activity of the *E. coli* replication origin, *oriC*. EMBO J. **4**:1327–1332.

18. **Nanninga, N., and C. L. Woldringh.** 1985. Cell growth, genome duplication, and cell division, p. 259–318. *In* N. Nanninga (ed.), Molecular cytology of *Escherichia coli*. Academic Press, Inc., New York.
19. **Nordström, K., S. Molin, and J. Light.** 1984. Control of replication of bacterial plasmids: genetics, molecular biology, and physiology of the plasmid R1 system. Plasmid **12**:71–90.
20. **Pato, M. L., P. M. Bennett, and K. von Meyenburg.** 1973. Messenger ribonucleic acid synthesis and degradation in *Escherichia coli* during inhibition of translation. J. Bacteriol. **116**: 710–718.
21. **Plank, L. D., and J. D. Harvey.** 1979. Generation time statistics of *Escherichia coli* B measured by synchronous culture techniques. J. Gen. Microbiol. **115**:69–77.
22. **Pritchard, R. H.** 1978. Control of DNA replication in bacteria, p. 1–26. *In* I. Molineux and M. Kohiyama (ed.), DNA synthesis, present and future. Plenum Publishing Corp., New York.
23. **Pritchard, R. H.** 1984. Control of DNA replication in bacteria, p. 19–27. *In* P. Nurse and E. Streiblová (ed.), The microbial cell cycle. CRC Press, Inc., Boca Raton, Fla.
24. **Pritchard, R. H., P. T. Barth, and J. Collins.** 1969. Control of DNA synthesis in bacteria. Symp. Soc. Gen. Microbiol. **19**:263–297.
25. **Rosenberger, R. F., N. B. Grover, A. Zaritsky, and C. L. Woldringh.** 1978. Surface growth in rod-shaped bacteria. J. Theor. Biol. **73**:711–721.
26. **Scott, J. R.** 1984. Regulation of plasmid replication. Microbiol. Rev. **48**:1–23.
27. **Shepard, H. M., D. H. Gelfand, and B. Polisky.** 1979. Analysis of a recessive plasmid copy number mutant: evidence for negative control of ColE1 replication. Cell **18**:267–275.
28. **Skarstad, K., E. Boye, and H. B. Steen.** 1986. Timing of initiation of chromosome replication in individual *Escherichia coli* cells. EMBO J. **5**:1711–1717.
29. **Sompayrac, L., and O. Maaløe.** 1973. Autorepressor model for control of DNA replication. Nature (London) New Biol. **241**: 133–135.
30. **Steen, H. B.** 1980. Further developments of a microscope-based flow cytometer: light scatter detection and excitation intensity compensation. Cytometry **1**:26–31.
31. **Steen, H. B.** 1983. A microscope-based flow cytometer. Histochem. J. **15**:147–160.
32. **Steen, H. B., and T. Lindmo.** 1979. Flow cytometry: a high-resolution instrument for everyone. Science **204**:403–404.
33. **Tomizawa, J., and T. Itoh.** 1981. Plasmid ColE1 incompatibility determined by interaction of RNA1 with primer transcript. Proc. Natl. Acad. Sci. USA **78**:6096–6100.
34. **Trueba, F. J.** 1982. On the precision and accuracy achieved by *Escherichia coli* cells at fission about their middle. Arch. Microbiol. **131**:55–59.
35. **Trueba, F. J., and C. L. Woldringh.** 1980. Changes in cell diameter during the division cycle of *Escherichia coli*. J. Bacteriol. **142**:869–878.
36. **Zaritsky, A.** 1975. Rate stimulation of deoxyribonucleic acid synthesis after inhibition. J. Bacteriol. **122**:841–846.
37. **Zaritsky, A., N. B. Grover, J. Naaman, C. L. Woldringh, and R. F. Rosenberger.** 1982. Growth and form in bacteria. Comments Mol. Cell. Biophys. **1**:237–260.